Isr. J. Earth Sci.; 54: 1–14

Temporal and spatial variations of microearthquake activity along the Dead Sea Fault, 1984–2004

Ze'ev B. Begin and Gideon Steinitz
Geological Survey of Israel, 30 Malkhe Yisrael Street, Jerusalem 95501, Israel

(Received 6 January 2004; accepted in revised form 28 October 2004)

ABSTRACT

Begin, Z.B. and Steinitz, G. 2005. Temporal and spatial variations of microearthquake activity along the Dead Sea Fault, 1984–2004. Isr. J. Earth Sci. 54: 1–14.

Patterns of spatial and temporal variations in microearthquake activity during 1984–2004 were studied in five segments along the Dead Sea Fault (DSF). In each segment there is a narrow zone in which intense seismic activity is concentrated; the most active one is the Dead Sea segment. Segments are also characterized by distributions of hypocenter depths, with the northern Arava and Dead Sea showing the deepest hypocenters.

The annual distribution of earthquakes is nonuniform in all segments, with years of peak activity occurring between 1989 and 1992 in the different segments. The maximum annual number for the DSF as a whole was 215 earthquakes ($M_L \geq 0$) in 1991, while in 1984 and in 2001 the number of earthquakes was only about 70. The cumulative seismic moment for the DSF decreased exponentially from 1984 ($2 \cdot 10^{22}$ dyne cm) to 20% of that value in 2003 and then increased by two orders of magnitude in 2004. During 1995–2004 the changes in the annual number of earthquakes were concomitant with changes in the average annual Rn concentration, as measured close to the active boundary fault in the NW Dead Sea. In southern Israel and Jordan, where only few earthquakes had occurred between 1984 and 1995, a marked increase in seismic activity took place after the 1995 Nuweiba earthquake in the Gulf of Elat.

INTRODUCTION

The Dead Sea Fault (Transform) is an active fault zone forming the Arabian–Sinai plate boundary, stretching from the spreading Red Sea to the Eastern Anatolian Fault. All along the Transform it is accompanied by a conspicuous rift valley. Based on considerations of plate kinematics and matching of structures across the Fault (summarized by Garfunkel, 2001), it is generally accepted that the principal sense of movement along the Fault has been left lateral, with a total slip of 105 km (Quennel, 1959; Freund, 1965; Freund et al., 1970; Garfunkel et al., 1981; Garfunkel, 2001). According to a different view, the horizontal slip along the Dead Sea fault is smaller (Mart, 1991; Horowitz, 2001), amounting to 10–20 km (Mart et al., 2005).

The average horizontal slip rate along the Dead Sea Fault (DSF) during the last 5 Ma was determined to be 6–7 mm/year, based on plate kinematics (Joffe and Garfunkel, 1987; Garfunkel, 2001). Along the middle and northern Arava segment of the DSF, several estimates of horizontal slip rates were suggested, based on

E-mail: begin_bz@mail.gsi.gov.il

 0021-2164/05 $4.00

displaced alluvial fans, terraces, and gullies: 3–7.5 mm/year during the last 5–2 Ma (Ginat et al., 1998); 4 ± 2 mm/year during the last 70,000–140,000 years and 5 ± 1.2 during the last 2,000–3,000 years (Klinger et al, 2000); 4.7 ± 1.3 mm/year during the last 15,000 years and 3.9 ± 0.5 during the last 6,000 years (Niemi et al., 2001). In the Missyaf segment of the DSF in Syria, north of the Yammuneh restraining bend, a displaced aqueduct shows a slip rate of 7 mm/year during the last 2000 years (Meghraoui et al., 2003). Based on GPS measurements, the current slip rate along the DSF is 3.3 ± 0.4 mm/year (Wdowinski et al., 2004).

A century-long record that includes strong earthquakes shows that the moment released by the observed earthquakes along the DSF did not account for more than 2 mm/year of the rate of relative motion across the Transform (Ben-Menahem, 1981; Garfunkel et al., 1981; Salamon et al., 2003; Shapira et al., 2004). Noting that in these calculations the moments were added regardless of the actual direction of movement on particular faults (Salamon et al., 2003), this is a maximum value. Deficiency in seismic moment along the Dead Sea Fault is also shown for the period 70–14 ky BP in the record of the Lisan Formation, by the meagerness of strong earthquakes (Marco et al., 1996; Begin et al., 2005), as well as in the record of damaged cave deposits in the Soreq Cave, 40 km west of the Dead Sea (Kagan et al., 2005). Thus, the seismic activity accounts for only a part of the movement along the DSF.

Of the earthquakes that occurred along the DSF in the last 20 years about 99% were of a magnitude <4, and one should be cognizant of the fact that the relationship between such small seismic events and the seismotectonic regime along the DSF is not at all obvious. This problem is examplified by the fact that in spite of the overwhelming evidence for a left-lateral movement along the DSF, several fault-plane solutions along it (carried out for $M_L \geq 4$ earthquakes) indicate other mechanisms and directions of movement, some attesting to normal faulting and hence extension in a direction perpendicular to the DSF direction. The expected main component of left-lateral motion on NNE-striking faults along the DSF is found in the fault-plane solutions for the strongest events, in 1927 and in 1995 and their aftershocks (Salamon et al., 2003). On top of these problems, the present study is based on an instrumental record that is only 21 years long and the limitations on the ability to draw pertinent tectonic information from this short period are clear. On the other hand, the importance of microearthquakes should not be dismissed hastily. Their analysis reveals regular patterns that are characteristic of tectonic provinces (Wesnouski, 1990; Stirling et al., 1996), and it has also been shown that a rise in the seismic rate of small earthquakes may herald a strong earthquake (Shapira, 1990; Bowman et al., 1998).

Time-dependent seismic behavior of strong earthquakes along the DSF has been shown on the scale of tens of thousands of years (Marco et al., 1996; Begin et al., 2005), thousands of years (Amit et al., 1995; Leonard et al., 1998; Zilberman et al., 2000; Amit et al., 2002), and hundreds of years (Migowski et al., 2004). Seismic characteristics of segments along the DSF, based on short records of microearthquakes, have been discussed previously (Wu et al., 1973; Arieh and Rotstein, 1985; Rotstein and Arieh, 1986; Shapira and Feldman, 1987; van Eck and Hofstetter, 1989, 1990; Hofstetter et al., 1996). However, these short-term analyses did not permit presentation of temporal patterns in the rate of seismic activity along the DSF.

Here we report temporal patterns in the rate of microearthquake seismicity on the scale of years, after two decades of meticulous data gathering of microearthquakes in this region by the Seismology Division of the Geophysical Institute of Israel.

METHOD

In some previous studies that addressed seismicity along the DSF, the area between the Gulf of Elat and the Baqaa in Lebanon was subdivided into two segments: a northern segment, which either includes the southern Dead Sea (Ben-Menahem, 1991; Yücemen, 1992) or excludes it (Khair et al., 2000), and the Arava segment. In other studies a more detailed subdivision was employed, based on geological considerations. Since the DSF comprises pull-apart grabens and segments between them that are structurally higher (Heimann, 1990; Garfunkel, 1997; Frieslander and Bartov, 1997), in the studied area the DSF lends itself to a natural subdivision into four segments (Arieh and Rabinowitz, 1989; Shamir et al., 2001): The Arava structural high, the Dead Sea pull-apart, the Jordan valley structural high, and the Kinneret–Hula pull-aparts. In an attempt to furnish more detail on the 120-km-long Arava segment, we divided it further into northern and southern segments with the border between them in the Arava water divide (Fig. 1).

The earthquake data set for the study area (Fig. 1) was taken from the Israeli earthquake catalog for 2004

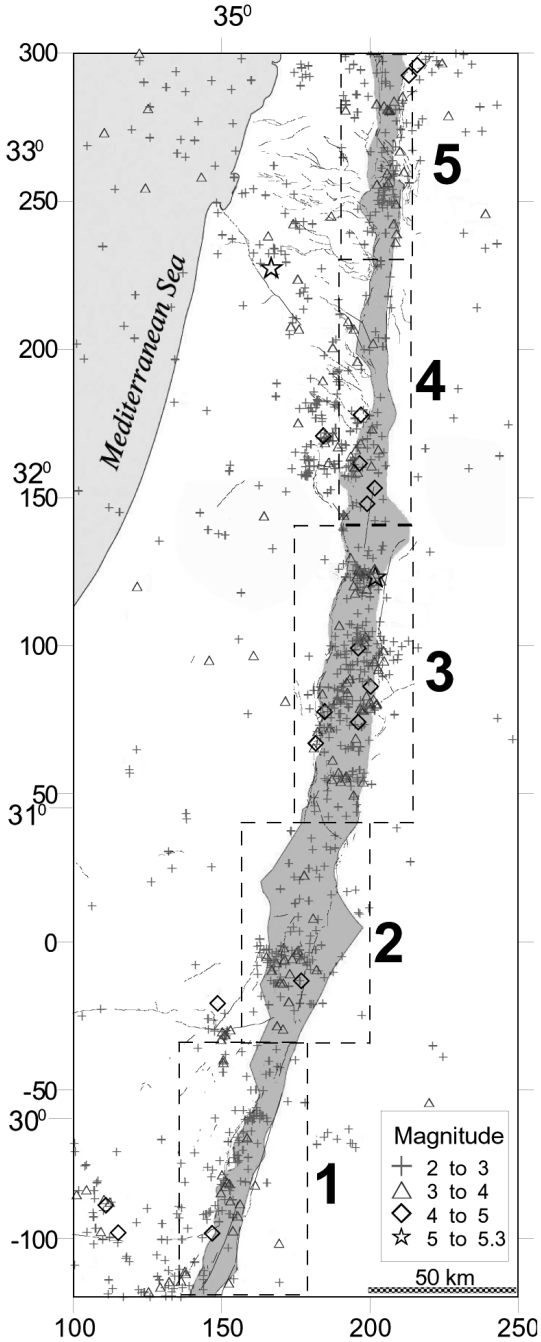

Fig. 1. Earthquakes ($M_L \geq 2$) during 1984–2004 along the DSF and near it, classified according to their magnitude (M_L), shown on the backdrop of faults that are potentially active (Bartov et al., 2002). Rectangles are segments used in this study; from bottom: (1) southern Arava (135/–120 to 175/–030), (2) northern Arava (155/–030 to 200/040), (3) Dead Sea (175/040 to 215/140), (4) Jordan Valley (190/140 to 215/230), (5) Kinneret (190/230 to 215/300). Grey area denotes the Dead Sea rift valley.

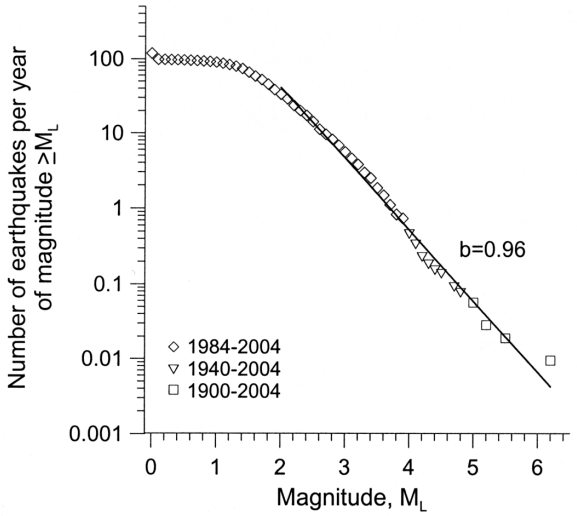

Fig. 2. Cumulative magnitude–frequency diagram for earthquakes in the five segments along the DSF (Fig. 1). Data are based on periods with complete records: since 1900 for $M_L \geq 5$, since 1940 for $M_L \geq 4$, and since 1984 for $M_L \geq 2$. The resulting b-value is 0.96.

(www.gii.co.il/html/seis/seis_search.html), as published by the Seismology Division of the Geophysical Institute of Israel, which operates the Israel Seismic Network (ISN). The magnitude threshold of complete record for the area along the DSF is, since 1986, $M_L \geq 2.0$ (Shapira, 1992); for 1984–1985 the threshold is $M_L \geq 2.5$ (Shapira, 2002, appendix A). Although the ISN was installed in 1980, the record analyzed here starts in 1984, taking into account initial difficulties in the ISN operation. The magnitude–frequency relationship (Fig. 2) shows that this study deals with microearthquakes.

The presentation of the results starts with general considerations: a description of the spatial distribution of earthquakes, the adequacy of the data set, and the temporal nonuniformity of the time series for the DSF as a whole. We then proceed to describe in each segment the temporal patterns of two aspects of seismicity: number of earthquakes and seismic moment.

RESULTS

A. General considerations

Spatial clusters

As already noted, on the basis of few years of observations (van Eck and Hofstetter, 1989, 1990; Shapira, 1990), the spatial distribution of microearthquakes along the DSF is nonuniform. Five spatial

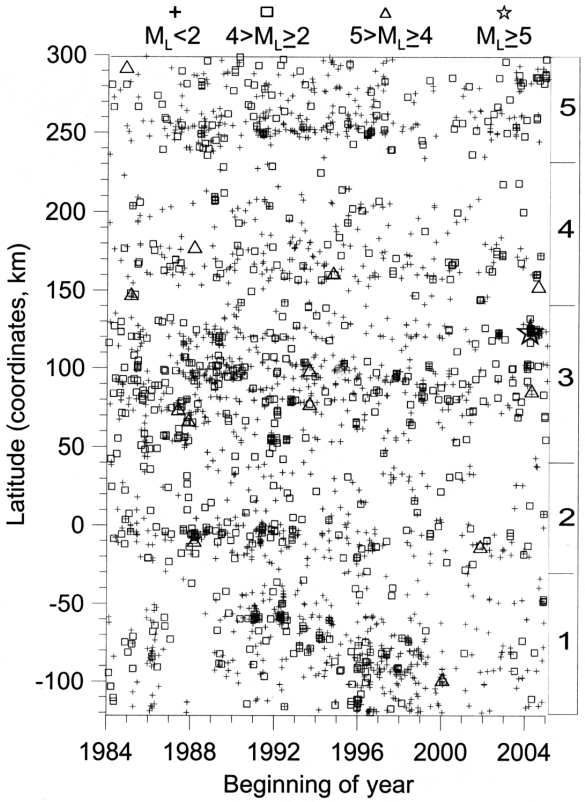

Fig. 3. A space–time diagram showing seismic activity along the DSF, 1984–2004, for all recorded earthquakes. Note clustering of earthquakes in narrow zones within each segment. Segment numbers in right-hand column correspond to Fig. 1.

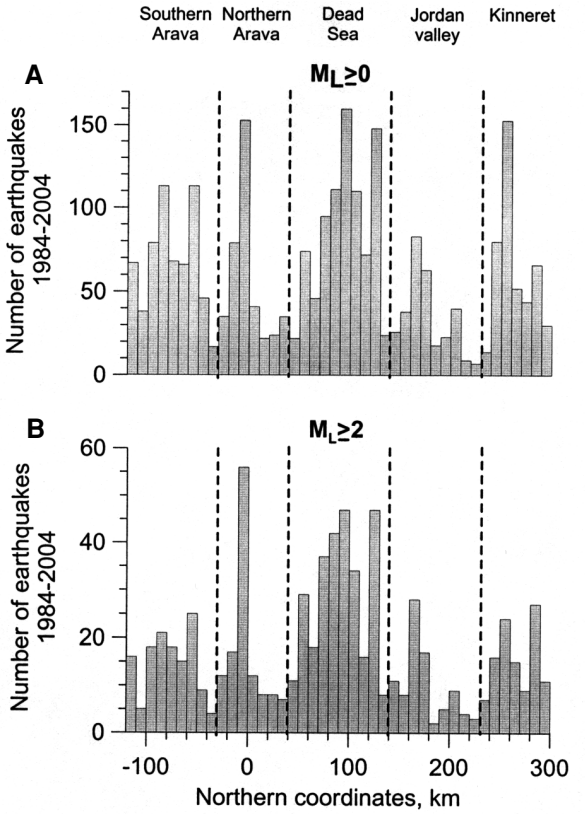

Fig. 4. Distribution of earthquakes along the DSF, for 1984–2004. Discussed segments are indicated. Bin size is 10 km. A: $M_L \geq 0$. B: $M_L \geq 2$. The figures are quite similar, but with the smaller earthquakes the clustering along the DSF is more pronounced.

clusters, one in each segment, are revealed in Figs. 3 and 4. Measured along the north–south direction, the width of these clusters comprises only some 10% of the rift length, but more than 20% of the earthquakes that occurred in 1984–2004 are concentrated in them. In the Arava, Dead Sea, and Jordan valley segments (Fig. 1) the locations of these clusters coincide with junctions of the DSF with transversal faults: The Thamad fault in the Southern Arava, the Paran–Arif fault in the northern Arava, an E–W fault east of the Dead Sea, and the Faria fault in the Shomeron (see also Aldersons et al., 2003, fig. 1).

The five segments also show characteristic distributions of hypocenter depths (Fig. 5), despite the large error in their determination and recognizing that depth was truncated in the determination algorithm at 25 km (A. Shapira, personal communication, 2004). Characterizing the depth distributions by their medians, the northern Arava and Dead Sea segments are similar (median depth = 11.5 km), the southern Arava has shallower hypocenters (median = 9.5 km), and the Jordan valley and Kinneret segments show still shallower hypocenters (median depths of 9 km and 7.5 km, respectively). The differences between the depth distributions of the northern Arava and Dead Sea segments and those of the three other segments are significant at the $p < 10^{-5}$ level (Fig. 5). Except for the southern Arava segment, this trend corresponds to the south-to-north thinning of the crust by 5 km along the DSF (Aldersons et al., 2003).

Earthquake doublets

Earthquake "doublets" are those that occur a short time (here defined as less than one day) after a previous earthquake. "Doublets" might spuriously affect the analysis of the annual number of earthquakes because some of them are dependent on the occurrence of earthquakes that immediately precede them. To ex-

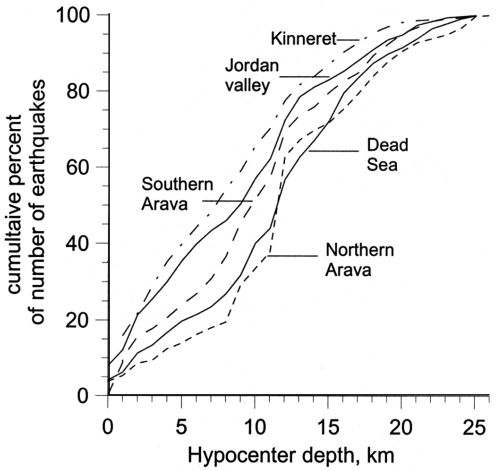

Fig. 5. Depth of hypocenters in the five segments along the DSF for the period 1984–2004, depicted by the cumulative percent of earthquakes in each segment. The differences between the depth distributions in the Dead Sea and northern Arava segments, with a median of 11.5 km, are significantly different ($p < 10^{-5}$, tested with the Mann–Whitney test) from the depth distributions in the segments of the Kinneret (median = 7.5 km), the Jordan valley (median = 9 km), and the southern Arava (median = 9.5 km).

amine this issue, the difference (T_p) between the occurrence time of an earthquake and the occurrence time of an immediate previous one was calculated, as well as the distance (D_p) between the locations of the two earthquake epicenters. The data set was subdivided into two subsets: one with T_p <1 day (Fig. 6A) and the other with $T_p \geq 1$ day (Fig. 6B). It is seen that for earthquakes with $T_p < 1$ day the modal D_p is 0–5 km. The same data set was further subdivided into D_p results in two different subsets: one with $D_p < 5$ km (Fig. 6C) and the other with $D_p \geq 5$ km (Fig. 6D). These subsets are quite distinct: Only 20% of earthquakes with $D_p \geq 5$ km occurred within $T_p < 0.5$ day, while about 70% of the earthquakes with $D_p < 5$ km occur within that time interval, indicating a correlation between consecutive earthquakes that occur within a short distance from previous ones. The percent of earthquakes with $D_p < 5$ km increases with the annual number of earthquakes (Fig. 7B).

Nonuniformity of the earthquake time series

Only earthquakes with $M_L \geq 2.0$ are fully represented in the catalog, and the percent of earthquakes

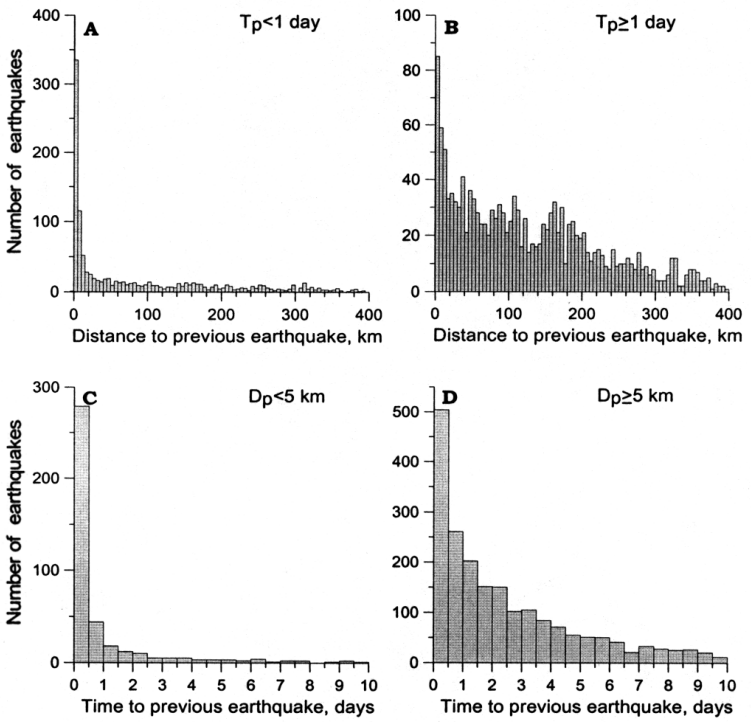

Fig. 6. For all earthquakes during 1984–2004 in the five segments along the DSF: A–B: Occurrence of distance to previous earthquake (D_p) for two different time intervals to previous earthquake (T_p). About 30% of earthquakes with $T_p < 1$ day are found at $D_p < 5$ km. Bin size is 5 km. C–D: Occurrence of time intervals to previous earthquakes (T_p) for two different distances to previous earthquake (D_p). About 70% of the earthquakes with $D_p < 5$ km have a $T_p < 0.5$ day, while for $D_p > 5$ km only 25% are within that time interval. Bin size is 0.5 day.

with $M_L < 2.0$ increases with the annual number of earthquakes (Fig. 7A). In the following analyses we included all earthquakes that are registered in the catalog, assuming that the total number provides an indicator for the seismic activity.

Considering only earthquakes with $M_L \geq 2.0$ and $D_p > 5$ km, which may be viewed as the "harder core" of the data, the temporal nonuniformity is obvious (Fig. 7C). For earthquakes with $M_L \geq 3.0$, the completeness of the record along the DSF allows us to extend the time series back to 1964 (Shapira, 2002). Although the total number of these earthquakes is small (Fig. 7D), it is possible to compare their numbers in the first 20 years of this period (1964–1983, 30 earthquakes) to the latter 20 years (1984–2003, 114 earthquakes, even without considering 2004 with its exceptionally high number of $M_L \geq 3.0$ earthquakes) and to test through the χ^2 test the probability of random occurrence of such deviation from the long-term average ($p < 0.0001$). We may conclude that on a decadal scale the nonuniformity of the time series of annual number of earthquakes is a real attribute of the seismic behavior along the DSF during the studied period.

B. Number of earthquakes

Annual distribution of earthquakes

Incorporating all earthquakes ($M_L \geq 0$) within the studied area, the time series for the different segments is presented in Fig. 8. In each of the segments, the distribution of earthquakes in time is significantly

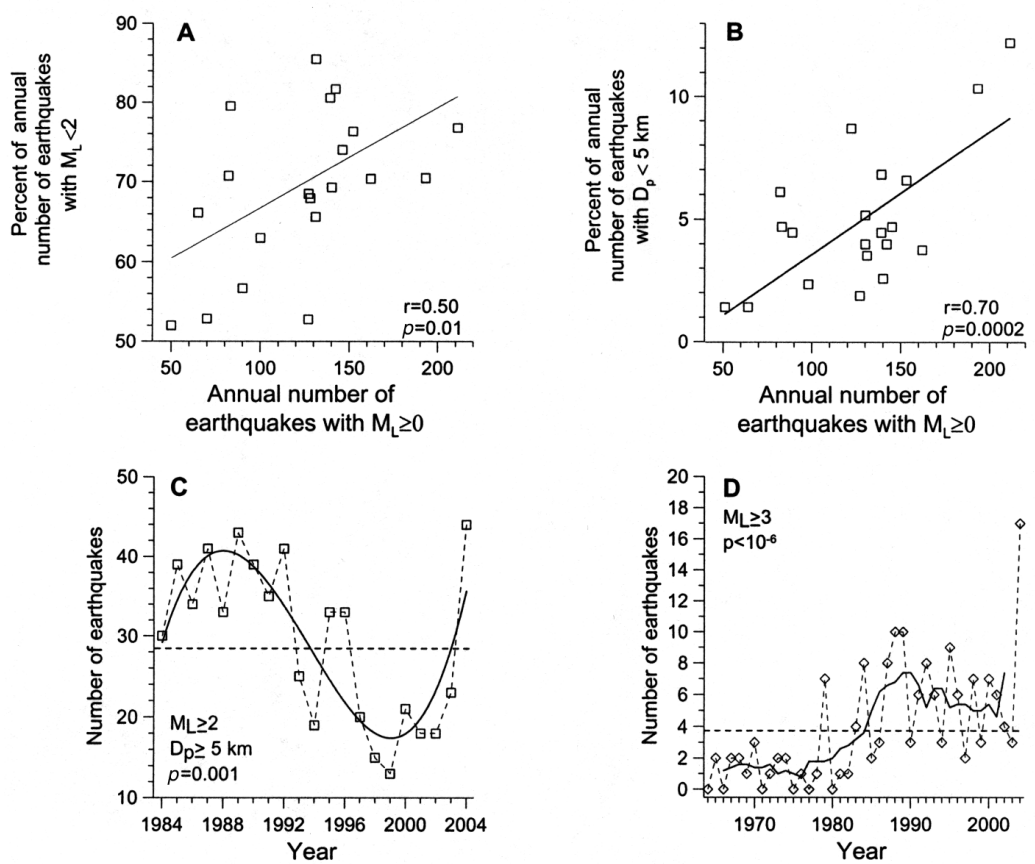

Fig. 7. For all segments. **A**: The increase in the percent of earthquakes having $M_L < 2$ with increasing annual number of earthquakes having $M_L \geq 0$ (1984–2004). *p* is the probability of random occurrence of the correlation coefficient r. **B**: The increase in the percent of earthquakes having $D_p < 5$ km with increasing annual number of earthquakes having $M_L \geq 0$ (1984–2004). **C**: The temporal nonuniformity of earthquake occurrence along the DSF, for earthquakes having $M_L \geq 2$ and $D_p \geq 5$ km. Cubic polynomial fit is statistically significant. Horizontal line shows the average for this period. **D**: The temporal nonuniformity of earthquake occurrence along the DSF, for the complete record of earthquakes having $M_L \geq 3$ for 1964–2004, with a 5-year running average. Horizontal line shows the average for this period.

different from a random one. The timing of the maxima of annual earthquake occurrence in the five segments changes slightly between 1989 and 1992; the maximum for the DSF as a whole is in 1991.

Earthquakes in the southern Arava and adjacent areas

After the 22 November 1995 Nuweiba earthquake (Shamir et al., 2003), a remarkable increase in seismicity is discerned, mainly NW and NE of Elat, more than 100 km north of the earthquake epicenter (Fig. 9). In these areas faults trending NW and NE, respectively, are not known. There was a marked increase in seismicity NW of Elat immediately after the Nuweiba earthquakes and a small increase in seismicity NE of Elat a year after that earthquake (Fig. 10), whereas in the southern Arava many earthquakes occurred before the Nuweiba earthquake. However, an increase in the number of earthquakes in the southern 50 kilometers of the Arava after the Nuweiba earthquake can be clearly seen in the bottom of Fig. 3. We propose that redistribution of stress following the Nuweiba earthquake is the cause of the increased seismicity in southern Israel and Jordan during 1995–1998.

Rate of seismicity and Rn concentration at the NW Dead Sea

Radon concentration has been measured near the western boundary fault in the northwestern Dead Sea since 1995. A statistically significant connection between anomalies in Rn concentration and earthquakes

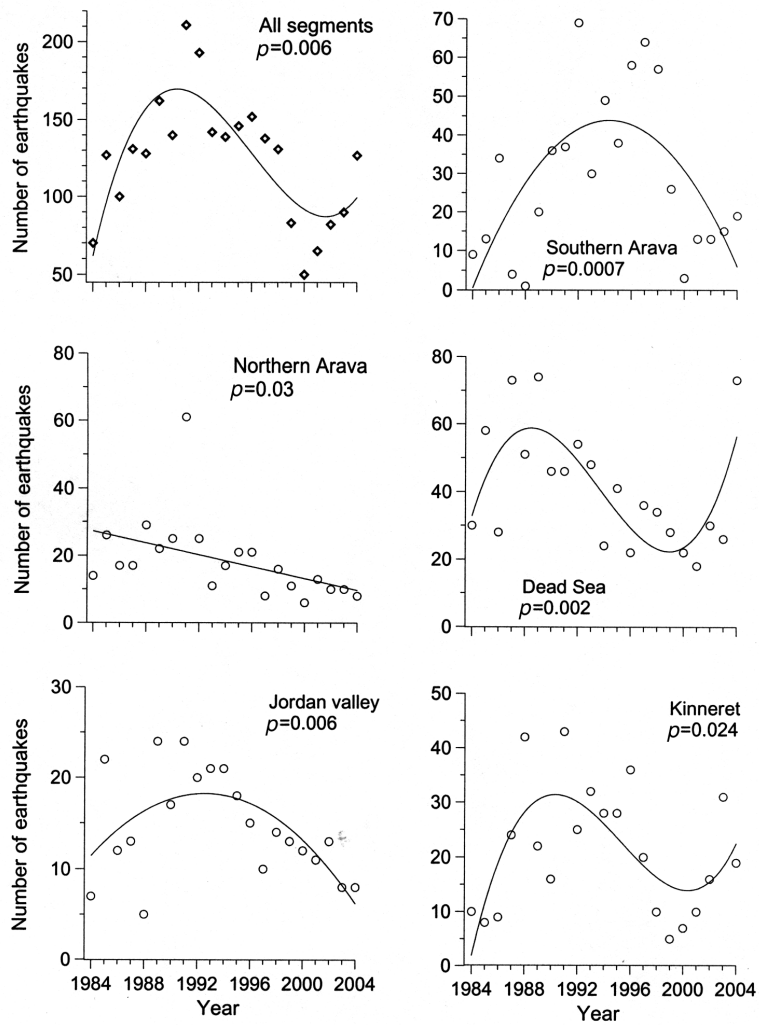

Fig. 8. Changes in the annual number of earthquakes ($M_L \geq 0$) along the DSF during 1984–2004. Temporal trends are illustrated through polynomial fits (quadratic polynomials for the southern Arava and Jordan valley segments, cubic polynomials for the Dead Sea and Kinneret segments, as well as for all segments together). *p* denotes the statistical significance of the fits.

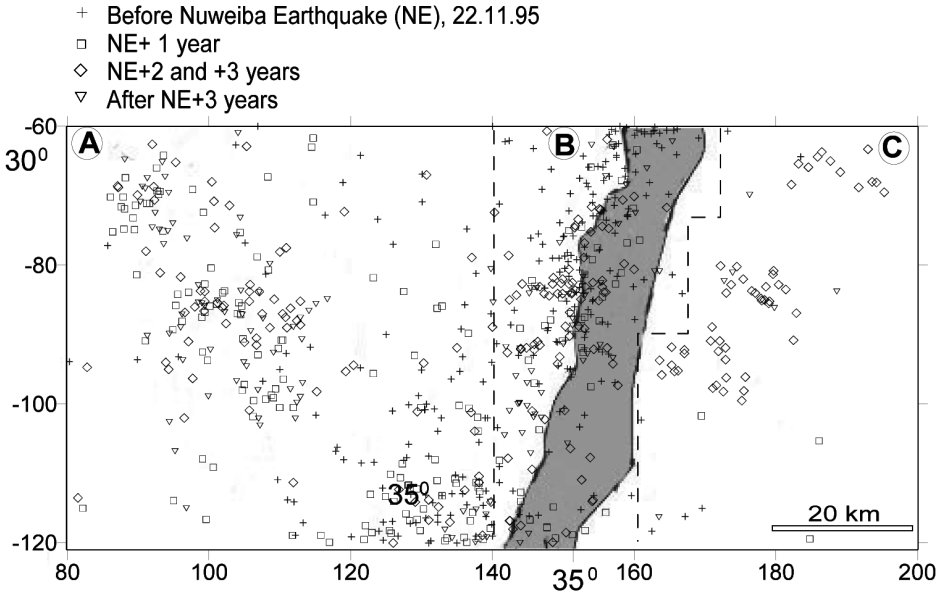

Fig. 9. Earthquakes ($M_L \geq 0$) in the southern Negev and Jordan for the period 1984–2004, classified according to their time of occurrence relative to the Nuweiba earthquake in the Gulf of Elat, 22 November 1995. Histograms of quarterly earthquake occurrence in areas A, B, and C are shown in Fig. 10. In areas A and C most earthquakes occurred after the Nuweiba earthquake.

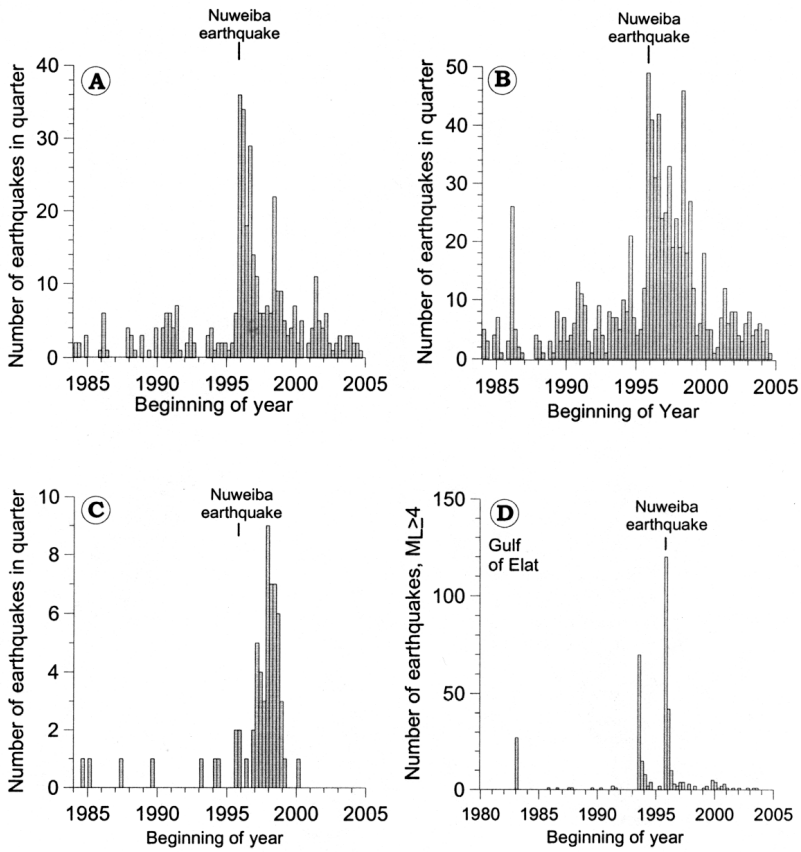

Fig. 10. A, B, C—quarterly earthquake ($M_L \geq 0$) occurrence in the three areas depicted in Fig. 9, respectively, showing an increase in the number of earthquakes after the Nuweiba 1995 earthquake in the Gulf of Elat. D—quarterly occurrence of earthquakes with $M_L \geq 4$ in the Gulf of Elat for the period 1980–2004.

in the Dead Sea and Kinneret basins has been presented (Steinitz et al., 2003). Here (Fig. 11), a statistically significant relationship between the annual number of earthquakes along the DSF and the annual average of Rn concentration is presented for the period 1995–2004. This correlation is quite remarkable, remembering that Rn concentration varies seasonally (Steinitz et al., 2003) and that the record pertains to only one station in the NW Dead Sea, while the number of earthquakes is recorded along the whole Dead Sea Fault, 200 km north and south of the Rn monitor (see also the Discussion below).

Seismic activity and fault offset

The seismic activity along five California strike-slip faults was shown to be inversely proportional to the overall fault displacement (Wesnousky, 1988). Seismic activity was measured as the number of earthquakes with $M_L \geq 3$ that occurred in 55 years per km of fault length, normalized per 1 mm of Holocene slip. In order to permit comparison to the DSF, seismicity is further normalized here per year, taking the DSF complete record for $M_L \geq 3$ of 41 years (1964–2004). The DSF fits well within the California scheme (Fig. 12).

C. Seismic moment

For 418 earthquakes in the area of study, seismic moment (M_0) values appear in the ISN catalog, being determined according to the method presented in Shapira and Hofstetter, 1993. These were used in order to estimate seismic moment for all other earthquakes studied here, by regressing log M_0 on magnitude, M_L (Fig. 13). For the range $0 \leq M_L \leq 5.2$ the relationship is well represented by the quadratic equation: $\log M_0 = 18.46 + 0.177\, M_L + 0.160\, M_L^2$. A similar relationship was found for California earthquakes (Hanks and Boore, 1984; Ben-Zion and Zhu, 2002), and for earthquakes in the DSF, the upward curvature of this non-linear relationship is implied by the findings of Hofstetter et al. (1996, fig. 7). From a linear regression of log seismic moment on earthquake magnitude, for the range $4 < M_L < 6.7$, Shapira and Hofstetter (1993) obtained the regression equation: $\log M_0 = (16.0 \pm 0.4) + (1.5 \pm 0.1)\, M_L$. This calculation underestimates the seismic moment of earthquakes with $M_L > 5.5$; for $M_L > 6$ it underestimates M_0 by more than 50%.

The annual seismic moment for the 425-km-long DSF studied here (Fig. 14) shows a significant exponential decrease during 1984–2003. On average, the cumulative seismic moment along the DSF in 2003 ($5.3 \cdot 10^{21}$ dyne cm) was only 20% of the seismic moment in 1984. For certain time intervals, in the Arava segments statistically significant ($p < 0.05$) exponential decrease in annual seismic moment release can be traced, while in the Kinneret segment an increase is discerned (Fig. 14); no trend is apparent in the Dead

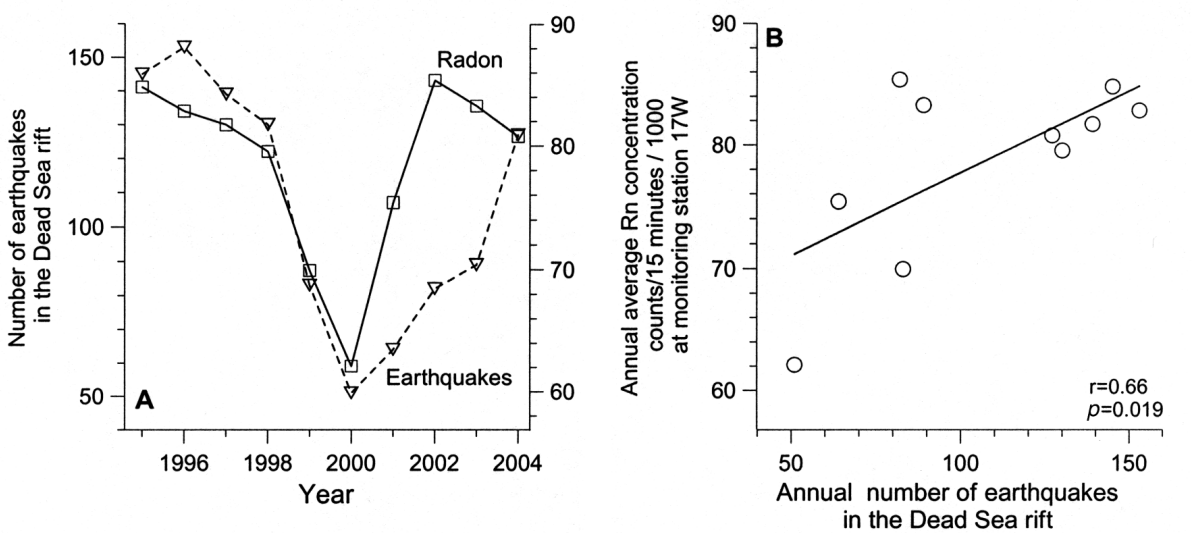

Fig. 11. A—Annual number of earthquakes ($M_L \geq 0$) in the DSF and annual average Rn concentration measured in the northwestern Dead Sea (Steinitz et al., 2003), 1995–2004. B—Correlation between annual number of earthquakes in the DSF and annual average Rn concentration measured in the northwestern Dead Sea. *p* is the probability of random occurrence of the correlation coefficient r.

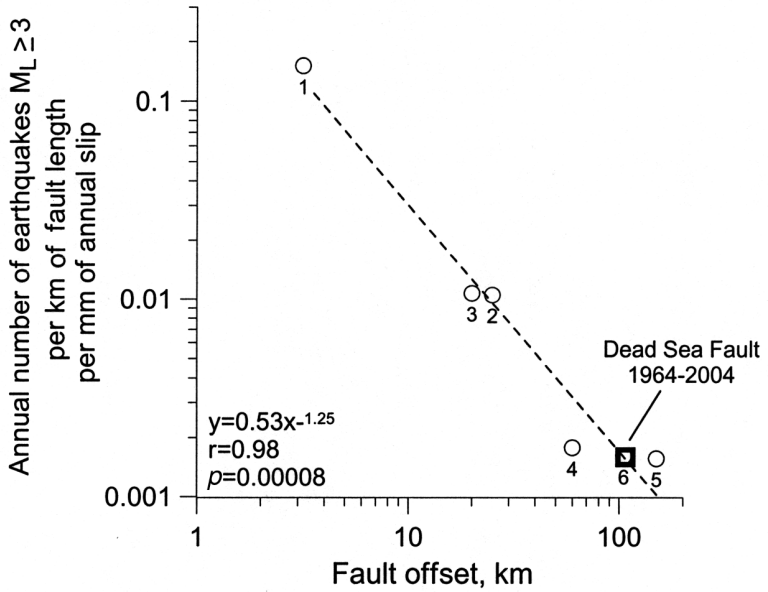

Fig. 12. The statistically significant correlation between fault offset and the annual number of earthquakes ($M_L \geq 3$) per km of fault length, normalized per 1 mm of annual slip rate, modified after a relationship originally proposed by Wesnouski (1990). Data points 1–5: Southern California strike-slip faults for 1932–1986 (Wesnousky, 1990). 1. Neweport-Inglewood. 2. San Jacinto. 3. Elsinore. 4. Garlock. 5. San Andreas. For (1) and (3), the offset is presented as the geometric mean of two extreme estimated values (Wesnousky, 1990, table 1). Data point 6: the Dead Sea strike-slip fault (1964–2004). *p* is the probability of random occurrence of the correlation coefficient r.

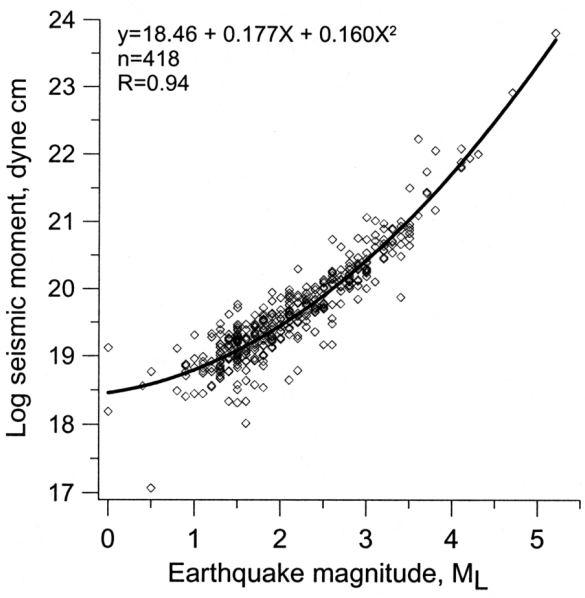

Fig. 13. The relationship between log seismic moment (dyne cm) and M_L as determined for 418 earthquakes in the five segments along the DSF (Fig. 1), showing a significant quadratic relationship.

Sea and Jordan valley segments. For the 21 years studied here, the cumulative seismic moment along the DSF is presented in Table 1, showing the change in the distribution of seismic moment between segments that took place after the $M_L = 5.2$ earthquake of 11.2.04.

DISCUSSION

The data presented above for 1984–2004 show some regularity in temporal trends in the seismic activity along the DSF, both in the annual number of earthquakes and in seismic moment. Although the centers of seismic activity in the five segments are 50–100 kilometers apart and the earthquakes are very small, the timing of the peaks of earthquake activity is similar, within a range of two years (1991–1992) in four of the five segments and within a range of four years (1989–1992) in all of the five segments. Simulating a random process, the probability was calculated of randomly obtaining a situation in which all five segments have their maximum number of earthquakes in any 4-year window within 21 years of measurements. The resulting probability is < 0.004 (we thank D. Steinberg

Table 1
Annual seismic moment (dyne cm) for the period 1984–2004

Segment (Fig. 1)	Annual average of seismic moment × 10^{22} dyne cm 1984–2003	Seismic moment × 10^{22} dyne cm during 2004
Southern Arava	0.2	0.05
Northern Arava	0.2	0.02
Dead Sea	0.4	66.5
Jordan valley	0.8	8.5
Kinneret	0.2	0.2

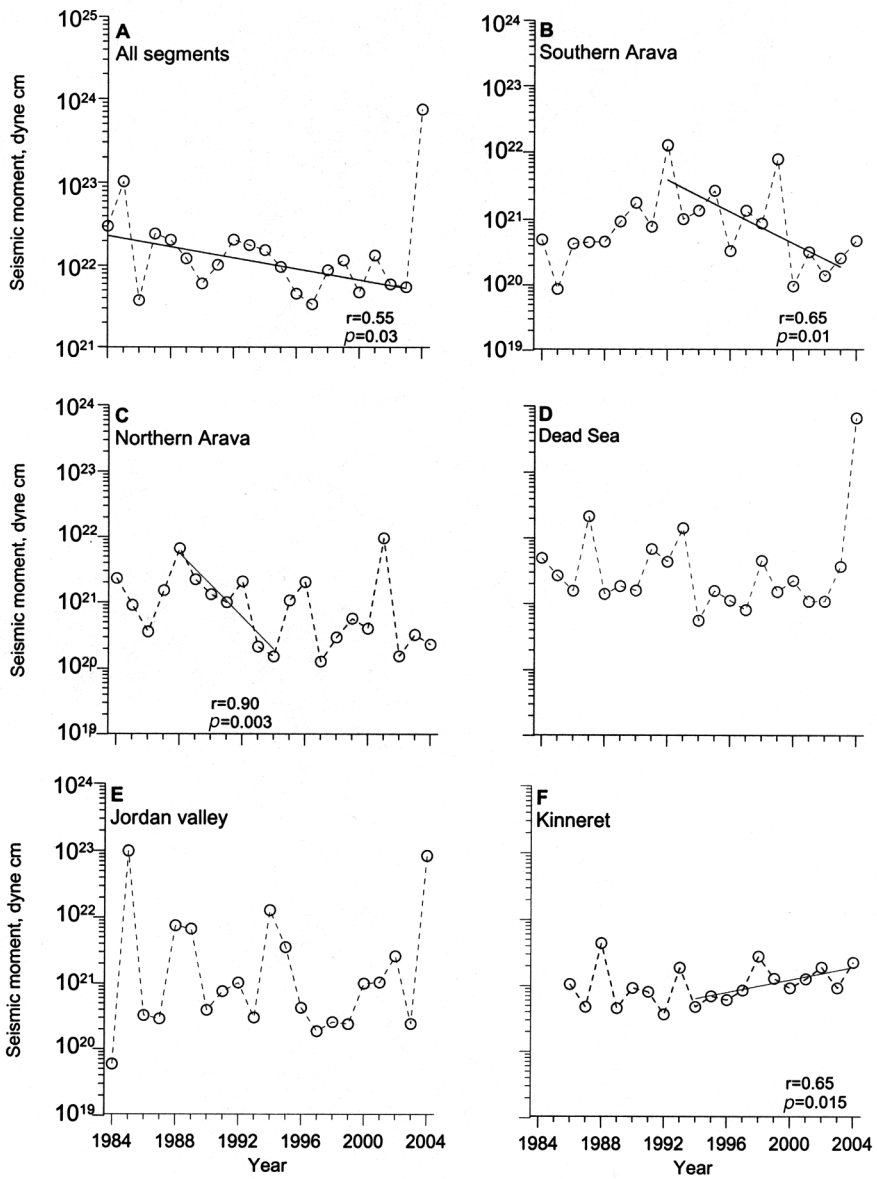

Fig. 14. Annual changes in seismic moment release (dyne cm) for 1984–2004. The lines show time intervals in which there is a statistically significant exponential change in seismic moment; *p* is the probability of random occurrence of correlation coefficient r. Note significant multi-year decrease in seismic moment for the DSF (Fig. 14A) during 1984–2003. Most of the seismic moment released in 2004 is due to M_L 5.2, 4.7, and 4.3 that occurred during February–July.

for the simulation). This indicates the operation of a mechanism that drives common earthquake activity along the DSF. This conclusion is supported by the gradual and consistent decrease of seismic moment for 20 years, during the period 1984–2003.

Such common mechanism is also indicated by the 10-year correlation between the annual number of earthquakes along the whole DSF and the average Rn concentration, as measured in one point, within the Dead Sea segment. It should be noted that many Rn anomalies in the Dead Sea area are not the result of earthquakes. Rather, they were shown to precede earthquakes and were interpreted as signifying transient stress along the DSF (Steinitz et al., 2003). Hence, a change in annual Rn concentration seems to indicate a change in the frequency of occurrence of stress transients. This leads us to assume that the decrease in number of earthquakes along the DSF during 1995–2000 and its increase during 2001–2004 do not signify an availability of fault planes that are ready to yield while the regional stress remains constant. Rather, they reflect general changes in stress.

As it is assumed that most of the smaller earthquakes along the DSF are an expression of normal faulting that is secondary to the main strike-slip movement on the DSF, it is intriguing to realize that their activity does reflect a large-scale tectonic process driven by a common source along the 400-km-long segment of the DSF.

The 20-year decrease in seismic moment and the decadal decrease in number of earthquakes along the DSF preceded the $M_L = 5.2$ earthquake in the NE Dead Sea on 11 February 2004. Its fault plane solution indicates that it probably did not occur on one of the main, N–S aligned, Dead Sea faults but on a plane that deviates 30° anticlockwise off the trend of the Transform (Salamon, 2004). This earthquake, the strongest one along the DSF since the $M_L = 5.5$ earthquake in the Dead Sea segment on 18.12.1956, released a seismic moment of $6.5 \cdot 10^{23}$ dyne cm, which is an order of magnitude greater than the cumulative seismic moment that had been released in the Dead Sea segment during the preceding 20 years. In hindsight, it may be that the gradual decrease in seismic activity along the DSF during 1991–2000, as well as the slight increase in seismic activity along the DSF after 1999 that could be discerned after 2003 (Fig. 7C), could have served as an indication for increasing probability of the occurrence of a strong earthquake after 2003.

The correlation between rate of seismicity (normalized to slip rate) and fault offset (Fig. 12) signifies a gradual process of decreased seismicity along the DSF on the scale of millions of years. For other faults, such decrease was explained by the continuous, long-term elimination of irregularities (Wesnouski, 1990; Stirling et al., 1996). Hence, the rate of seismicity along strike-slip faults evolves with time, and we may now apply this analysis to the Dead Sea Fault as well. This long-term evolution of seismicity means that the present seismic activity along a strike-slip fault system is the result of both its initial fault pattern and the unidirectional slow process through which it becomes less complex, with earthquakes converging towards its main faults (Ben-Zion et al., 1999). This means that the present seismicity of these strike-slip faults is affected by their past.

ACKNOWLEDGMENTS

Helpful suggestions by G. Baer, Y. Ben Zion, A. Hofstetter, V. Lyakhovsy, A. Shapira, and A. Salamon are gratefully acknowledged. Comments by two anonymous reviewers contributed much to the improvement of the manuscript. We thank D. Steinberg for his help with some statistical aspects of the study. We are grateful to L. Feldman for her effective asstance.

REFERENCES

Aldersons, F., Ben-Avraham, Z., Hofstetter, A., Kissling, E., Al-Yazjeen, T. 2003. Lower-crustal strength under the Dead Sea basin derived from local earthquake data and rheological modeling. Earth and Planetary Science Letters 214: 129–142.

Amit, R., Harrison, J.B.J., Enzel, Y. 1995. Use of soils and colluvial deposits in analyzing tectonic events—the southern Arava rift, Israel. Geomorphology 12: 91–107.

Amit, R., Zilberman, E., Enzel, Y., Porat, N. 2002. Paleoseismic evidence for time dependency of seismic response on a fault system in the southern Arava valley, Dead Sea rift, Israel. Geological Society of America Bulletin 114: 192–206.

Arieh, E., Rabinowitz, N. 1989. Probabilistic assessment of earthquake hazard in Israel. Tectonophysics 167: 223–233.

Arieh, E., Rotstein, Y. 1985. A note on the seismicity of Israel (1900–1982). Bulletin of the Seismological Society of America 75: 881–887.

Bartov, Y., Sneh, A., Fleischer, L., Arad, V., Rosensaft, M. 2002. Potentially active faults in Israel. Geological Survey of Israel Report GSI/29/2002, 8 pp.

Begin, Z.B., Steinberg, D.M., Ichinose, G.A., Marco, S.A. 2005. A 40,000 year unchanging seismic regime in the Dead Sea rift. Geology 33: 257–260.

Ben-Menahem, A. 1981. Variation of slip and creep along

the Levant Rift over the past 4500 years. Tectonophysics 80: 183–197.

Ben-Menahem, A. 1991. Four thousand years of seismicity along the Dead Sea rift. Journal of Geophysical Research 96B: 20,195–20,216.

Ben-Zion, Y., Dahmen, K., Lyakhovsky, V., Ertas, D., Agnon, A. 1999. Self-driven mode switching of earthquake activity on a fault system. Earth and Planetary Science Letters 172: 11–21.

Ben-Zion, Y., Zhu, L. 2002. Potency-magnitude scaling relations for southern California earthquakes with $1.0 < M_L < 7.0$. Geophysical Journal International 148: F1–F5.

Bowman, D.D., Ouillon, G., Sammis, C.G., Sornette, A., Sornette, D. 1998. An observational test of the critical earthquake concept. Journal of Geophysical Research 103B: 24,359–24,372.

van Eck, T., Hofstetter, A. 1989. Microearthquake activity in the Dead Sea region. Geophysical Journal International 99: 605–620.

van Eck, T., Hofstetter, A. 1990. Fault geometry and spatial clustering of microearthquakes along the Dead Sea–Jordan rift fault zone. Tectonophysics 180: 15–17.

Freund, R. 1965. A model of the structural development of Israel and adjacent areas since upper Cretaceous times. Geological Magazine 102: 189–205.

Freund, R., Garfunkel, Z., Zak, I., Goldberg, M., Weissbrod, T., Derin, B. 1970. The shear along the Dead Sea rift. Philosophical Transactions of the Royal Society of London, A 267: 107–130.

Frieslander, U., Bartov, Y. 1997. The structure of the Arava—new results from geological and geophysical studies. In: The Dead Sea rift as a Unique Global Site. 13th GIF Meeting, Terra Nostra.

Garfunkel, Z. 1997. The history and formation of the Dead Sea basin. In: Niemi, M., Ben Avraham, Z., Gat, J.R., eds. The Dead Sea, the lake and its setting. Oxford University Press, New York, pp. 36–56.

Garfunkel, Z. 2001. The nature and history of motion along the Dead Sea. In: Horowitz, A., ed. The Jordan rift valley. A.A. Balkema Publishers, Tokyo, pp. 627–651.

Garfunkel, Z., Zak, Y., Freund, R. 1981. Active faulting in the Dead Sea rift. Tectonophysics 80: 1–26.

Ginat, H., Enzel, Y., Avni, Y. 1998. Translocated Plio-Pleistocene drainage systems along the Arava fault of the Dead Sea transform. Tectonophysics 284: 151–160.

Hanks, T.C., Boore, D.M. 1984. Moment–magnitude relations in theory and practice. Journal of Geophysical Research 89: 6229–6235.

Hofstetter, A., Shapira, A., van Eck, T. 1996. Seismic activity along fault branches of the Dead Sea–Jordan transform system: the Carmel–Tirtza fault system. Tectonophysics 267: 317–330.

Horowitz, A. 2001. The Jordan rift valley. A.A. Balkema Publishers, Tokyo, 730 pp.

Joffe, S., Garfunkel, Z. 1987. Plate kinematics of the circum Red Sea—a re-evaluation. Tectonophysics 141: 5–22.

Kagan, E.J., Agnon, A., Bar-Matthews, M., Ayalon, A. 2005. Dating large infrequent earthquakes by cave deposits. Geology 33: 261–264.

Khair, K., Karakaisis, G.F., Papadimitrou, E.E. 2000. Seismic zonation of the Dead Sea transform fault area. Annali di Geofisica 43: 61–79.

Klinger, Y., Avouac, J.P., Abou Karaki, N., Dorbath, L., Bourles, D., Reyss, J.L. 2000. Slip rate on the Dead Sea transform fault in northern Araba valley (Jordan). Geophysical Journal International 142: 755–768.

Leonard, G., Steinberg, D.M., Rabinowitz, N. 1998. An indication of time-dependent seismic behavior—an assessment of paleoseismic evidence from the Arava Fault. Bulletin of the Seismological Society of America 88: 767–776.

Marco, S., Stein, M., Agnon, A., Ron, H. 1996. Long-term earthquake clustering: a 50,000-year paleoseismic record in the Dead Sea Graben. Journal of Geophysical Research 101B: 6179–6191.

Mart, Y. 1991. The Dead Sea rift: from continental rift to incipient ocean. Tectonophysics 197: 155–179.

Mart, Y., Ryan, W.B.F., Lunina, O.V. 2005. Review of the tectonics of the Levant Rift system: the structural significance of oblique continental breakup. Tectonophysics 395: 209–232.

Meghraoui, M. et al. 2003. Evidence for 830 years of seismic quiescence from palaeoseismology, archaeoseismology and historic seisimicity along the Dead Sea fault in Syria. Earth and Planetary Science Letters 210: 35–52.

Migowski, C., Agnon, A., Bookman (Ken-Tor), R., Negendank, J.F.W., Stein, M. 2004. Recurrence pattern of Holocene earthquakes along the Dead Sea Transform revealed by varve-counting and radiocarbon dating of lacustrine sediments. Earth and Planetary Science Letters 222: 301–314.

Niemi, T.M., Zhang, H., Atallah, M., Harrison, B.J. 2001. Late Pleistocene and Holocene slip rate in the Northern Wadi Araba fault, Dead Sea Transform, Jordan. Journal of Seismology 5: 449–474.

Quennel, A.M. 1959. Tectonics of the Dead Sea rift. 20th International Geological Congress, Mexico, pp. 385–405.

Rotstein, Y., Arieh, E. 1986. Tectonic implications of a recent microearthquake data from Israel and adjacent areas. Earth and Planetary Science Letters 78: 237–244.

Salamon, A. 1993. Seismotectonic analysis of earthquakes in Israel and adjacent areas. Ph.D. thesis, Hebrew Univ., Jerusalem, 135 pp. (in Hebrew, English abstr.).

Salamon, A. 2004. Seismically induced ground effects of the February 11, 2004, $M_L = 5.2$, northeastern Dead Sea earthquake. Geological Survey of Israel Report GSI/30/04, 25 pp.

Salamon, A., Hofstetter, A., Garfunkel, Z., Ron, H. 1996. Seismicity of the eastern Mediterranean region: perspective from the Sinai subplate. Tectonophysics 263: 293–305.

Salamon, A., Hofstetter, A., Garfunkel, Z., Ron, H. 2003.

Seismotectonics of the Sinai subplate—the eastern Mediterranean region. Geophysical Journal International 155: 149–173.

Shamir, G., Baer, G., Hofstetter, A. 2003. Three-dimensional elastic earthquake modeling based on integrated seismological and InSAR data: the Mw = 7.2 Nuweiba earthquake, gulf of Elat/Aqaba 1995 November. Geophysical Journal International 154: 731–744.

Shamir, G., Bartov., Y., Sneh, A., Fleischer, L., Arad, V., Rosensaft, M. 2001. Preliminary seismic zonation in Israel. Israel Geological Survey Report GSI/12/2001 and the Israel Geophysical Institute Report 550/95/01, 10 pp.

Shapira, A. 1990. Increasing seismicity as an earthquake precursor in Israel. Geophysical Journal International 101: 203–211.

Shapira, A. 1992. Detectability of regional seismic networks: analysis of the Israel Seismic Networks. Israel Journal of Earth Sciences 41: 21–25.

Shapira, A. 2002. An updated map of peak ground accelerations for the Israel Standard 413. The Geophysical Institute of Israel, Report 592/230/02 (in Hebrew, English appendixes).

Shapira, A., Feldman, L. 1987. Microseismicity of three locations along the Jordan rift. Tectonophysics 141: 89–94.

Shapira, A., Hofstetter, A.. 1993. Source parameters and scaling relationships of earthquakes in Israel. Tectonophysics 217: 217–226.

Shapira, A., Abdallah, A.F., Dabbeek, J., Hays, W. 2004. Earthquake hazard assessments for building codes. The Geophysical Institute of Israel Report 537/059/04, 30 pp.

Steinitz, G., Begin, Z.B., Gazit–Yaari, N. 2003. Statistically significant relation between Rn flux and weak earthquakes in the Dead Sea rift valley. Geology 31: 505–508.

Stirling, M.W., Wesnousky, S.G., Shimazaki, K. 1996. Fault trace complexity, cumulative slip, and the shape of the magnitude-frequency distribution for strike-slip faults: a global survey. Geophysical Journal International 124: 833–868.

Wdowinski, S., Bock, Y., Baer, G., Prawirodirdjo, L., Bechor, N., Naman, S., Knafo, R., Forrai, Y., Melzer, Y. 2004. GPS measurements of current crustal movements along the Dead Sea fault: Journal of Geophysical Research 109, BO5403: 1–16.

Wesnousky, S.G. 1990. Seismicity as a function of cumulative geologic offset: some observations from southern California. Bulletin of the Seismological Society of America 80: 1374–1381.

Wu, F.T., Karcz, I., Arieh, E., Kafri, U., Peled, U. 1973. Microearthquakes along the Dead Sea rift. Geology 1: 159–161.

Yücemen, M.S. 1992. Seismic hazard maps for Jordan and vicinity. Natural Hazards 6: 201–226.

Zilberman, E., Amit, R., Heiman, A., Porat, N. 2000, Changes in Holocene paleoseismic activity in the Hula pull-apart basin, Dead Sea rift, northern Israel. Tectonophysics 321: 237–252.